EVALUATION AND INVENTORY OF EMISSIONS FROM A BI-FUEL TURBO-CHARGED ENGINE OPERATING WITH MIXTURES OF CNG WITH H_2G AND BIOMETHANE WITH H_2G USING A PHENOMENOLOGICAL MODEL

Jullyane Raquel Almeida Nunes[a*], Felipe Diniz da Silva [b], Ana Paula Mattos [c], Christian Jeremi Coronado Rodriguez[d]

Federal University of Pará
[a*]jullyane.anunes@gmail.com[1] felipe.diniz.silva@itec.ufpa.br[2] mattos.ufpa@gmail.com[3], christian@unifei.edu.br

ARTICLE INFO

Keywords: *SI, emissions inventory, biomethane, green hydrogen.*

Received: Apr 28, 2025
Reviewed: May 08, 2025
Accepted: May 10, 2025

ABSTRACT

In Brazil and globally, the pursuit of alternative energy sources is intensifying, with biofuels emerging as a robust solution to achieve energy independence and reduce reliance on oil. Integrating biomethane and green hydrogen into compressed natural gas (CNG) is crucial for enhancing efficiency and cutting emissions. This combination offers significant benefits such as CO_2 reduction, improved combustion efficiency, and enhanced engine performance, promising a sustainable energy pathway. This study aims to predict CO and NOx emissions from a bi-fuel engine using a phenomenological model. It compares engine performance on CNG alone versus CNG with added H_2G and biomethane with H_2G. Experimental data from CNG operations are used initially, with subsequent simulations incorporating biomethane and H_2G blends. The phenomenological model employs the double Wiebe function to analyze energy release and the Stikey model for heat transfer calculations in gaseous fuels. Emissions calculations use the extended Zeldovich model for NO_x and the Ranggi model for CO. An emissions inventory using the BRAVES® model assesses applicability in the Brazilian context, combining top-down methods with fleet and fuel characteristics. The study underscores biomethane's potential to reduce NOx emissions but notes its tendency to increase CO levels, suggesting blending with H_2G as a viable solution for improved engine performance and emissions control in light vehicles.

1. INTRODUCTION

The transportation sector plays a crucial role in global mobility for people and goods, characterized by access to various modes such as road, rail, maritime, and air transport. However, its near-exclusive dependence on petroleum- derived fuels necessitates urgent decarbonization. In 2023, according to Empresa de Pesquisa Energética (2024), the sector accounted for 33% of national energy demand, with petroleum derivatives contributing significantly at 77.4% of this massive consumption. Reducing greenhouse gas (GHG) emissions, predominantly CO_2, from transportation is essential for meeting global climate targets, including a 45% reduction in emissions by 2030 compared to 2010 levels.

Global GHG emissions are a central concern in the fight against the current climate crisis. In 2023, the transportation sector emitted 217 megatons of CO_2, representing a 0.8% increase compared to 2022. The adoption of biofuels and waste, which constitute 22.5% of the sector's energy matrix, plays a crucial role in reducing these emissions (Empresa de Pesquisa Energética, 2024). From 2014 to 2023, there was a significant 4.9% increase in renewable fuels. Biofuels offer a renewable and sustainable alternative to fossil fuels, helping to keep global warming below 1.5°C, as established by the Paris Agreement (Urroz *et al.*, 2023).

In the search for sustainable alternatives, hydrogen stands out as a promising fuel due to its unique characteristics, such as a rapid combustion rate and zero carbon emissions, depending directly on how it is produced. Hydrogen can be produced through sustainable processes, such as water electrolysis using renewable energy, resulting in zero carbon emissions during its use. This contrasts with traditional fuels, whose carbon emissions are intrinsically linked to their combustion process (Li *et*

* Corresponding author: Jullyane Raquel Almeida Nunes. Federal University of Pará. jullyane.anunes@gmail.com

al., 2024). Its use as an additive to gasoline has shown significant results in internal combustion engines. Studies demonstrate that hydrogen enrichment in the mixture tends to increase indicated thermal efficiency (ITE) while reducing specific fuel consumption. Additionally, it contributes to more stable combustion, resulting in higher peak pressure in the cylinder and lower variability between cycles. Although emissions of HC and CO are reduced, there is an observed increase in NO_x emissions with the addition of hydrogen to the mixture, although the engine's combustion limit is expanded, allowing greater operational flexibility (Li *et al.*, 2024).

Hydrogen also stands out as a viable additive for natural gas engines undergoing lean combustion due to its high laminar flame speed and wide flammability range. Adding hydrogen to methane, for example, improves combustion speed and increases engine efficiency while reducing CO_2 and HC emissions. This mixture offers the possibility to operate with leaner mixtures, which is advantageous for load control strategies. However, it is important to adjust the ignition timing to avoid knocking issues, which may occur due to the higher combustion speed and higher temperatures of the burned gases (Li *et al.*, 2024).

Numerical modeling of engines has become fundamental in the development of internal combustion engines, especially given the growing variety of design parameters and alternative fuels available. This method allows simulating complex scenarios throughout the engine cycles, incorporating fluid dynamics, heat transfer, thermodynamics, and chemical kinetics to accurately predict combustion, emissions, and operational performance. Creating mathematical models for engine simulation requires refined empirical correlations and approximations derived from detailed experimental studies. Such models are categorized in terms of thermodynamics and fluid dynamics, where energy and momentum equations are solved within a specific flow domain (Yıldız and Albayrak Çeper, 2017).

Therefore, this study aims to compare in detail the performance of the engine using a mixture of CNG and H_2, as well as biomethane with added H_2, employing a phenomenological model adapted from Mattos (2018). Additionally, a comprehensive vehicle emissions inventory will be developed using the BRAVES® model to assess its specific applicability in the Brazilian context. The primary focus of the research will be to investigate the impact of replacing CNG with biomethane not only on pollutant gas emissions but also on essential engine performance parameters, providing fundamental information for future policies and sustainable energy strategies in the transportation sector.

2. METHODOLOGY

The engine under analysis is a turbocharged, bi-fuel engine used in light vehicles and operating with CNG. The study evaluates the results of volumetric and thermal efficiency, torque, power, and peak pressure. Two engine speeds (2500 and 3000 rpm) were defined for the study, using the stoichiometric excess air coefficient (λ = 1) under full load conditions. The fuels analyzed in this work consist of the natural gas marketed in the southern region of the state of Minas Gerais and the biomethane produced by a company in the state of Rio de Janeiro, with the addition of H_2. The engine geometry data are presented in Table 1.

Table 1. Engine specifications

Specification	Specification value
Engine Type	Turbocharged, bi-fuel Spark Ignition Engine (SI)
Number of Cylinders	4
Cylinder Diameter [mm]	95.8
Stroke [mm]	104
Connecting Rod Length [mm]	158
Compression Ratio	12.5
Displacement Volume [cm^3]	749.64
Dead Volume [cm^3]	65.18
Intake Valve Diameter [mm]	29.07
Exhaust Valve Diameter [mm]	29.07

In the phenomenological model of Mattos (2018), the double Wiebe function was implemented to find the mass fraction burned as a function of the crank angle, which shows better convergence. The Stikey model was used to calculate the film coefficient for predicting heat transfer for gaseous fuels. This model was chosen because a previous study was conducted to analyze which model in the literature best represented the phenomenon with gaseous fuels. NO_x emissions are calculated using the extended Zeldovich model, and CO emissions are calculated using the Ranggi model. The parameters were used to carry out an emissions inventory using the BRAVES® model, which combines the top-down method with fleet and fuel characteristics.

2.1 Fuel Modeling

In the original model, two types of fuels were implemented: CNG and biomethane with additions of H_2.

Initially, a polynomial was developed covering the temperature range from 298K to 2000K. This polynomial created for methane, shown in Equation 1, used the Lagrange polynomial interpolation method in the Matlab® development environment.

This method proved to converge more efficiently with the phenomenological model in question. The same methodology was used for ethane (Eq. 2), propane (Eq. 3) and butane (Eq. 4).

$$C_{p,CH4} = aT^{17} + bT^{16} + cT^{15} + dT^{14} + eT^{13} + \\ + f\ T^{12} + gT^{11} + hT^{10} + iT^{9} + jT^{8} + kT^{7} + \\ + lT^{6} + mT^{5} + ... + qT + r \quad (1)$$

$$C_{p,C2H6} = aT^{8} + bT^{7} + cT^{6} + dT^{5} + eT^{4} + \\ + f\ T^{3} + gT^{2} + hT^{1} + i \quad (2)$$

$$C_{p,C3H8} = aT^{12} + bT^{11} + cT^{10} + dT^{9} + eT^{8} + \\ + f\ T^{7} + gT^{6} + hT^{5} + iT^{4} + jT^{3} + kT^{2} + \\ + lT^{1} + m \quad (3)$$

$$C_{p,C4H10} = aT^{13} + bT^{12} + cT^{11} + dT^{10} + eT^{9} + \\ + f\ T^{8} + gT^{7} + hT^{6} + iT^{5} + jT^{4} + kT^{3} + \\ + lT^{2} + mT^{1} + n \quad (4)$$

The coefficients of the polynomial equations are presented in the Table 2.

Table 2. Coefficients C_p for CH_4, C_2H_6, C_3H_8 and C_4H_{10}.

Coefficients	*CH_4*	*C_2H_6*	*C_3H_8*	*C4H10*
a	-5.866×10^{-14}	-1.329×10^{-33}	7.233×10^{-16}	-2.803×10^{-36}
b	1.158×10^{-11}	1.456×10^{-29}	-3.805×10^{-15}	3.228×10^{-32}
c	-1.061×10^{-9}	-7.193×10^{-26}	8.580×10^{-12}	-1.689×10^{-28}
d	5.996×10^{-8}	2.115×10^{-22}	-1.088×10^{-8}	5.314×10^{-25}
e	-2.338×10^{-6}	-4.123×10^{-19}	8.466×10^{-9}	-1.120×10^{-21}
f	6.668×10^{-5}	-5.602×10^{-16}	-4.114×10^{-6}	1.671×10^{18}
g	−0.00144	-5.430×10^{-13}	1.159×10^{-6}	-1.812×10^{-15}
h	0.0240	3.791×10^{-10}	-2.643×10^{-6}	1.445×10^{-12}
i	−0.314	-1.880×10^{-7}	1.988×10^{-5}	-8.479×10^{-10}
j	3.216	6.488×10^{-5}		3.607×10^{-7}
k	−25.878	−0.014		-0.108×10^{-3}
l	162.357	2.265		0.021
m	−783.748	−120.508		−2.246
n	2847.063			147.948
o	−7508.321			
p	13532.974			
q	−14866.436			
r	7516.056			

The results of volumetric and thermal efficiency, torque, power, and peak pressure are evaluated. The engine geometry data are presented in Table 3.

Table 3. Composition of Biomethane for Different Percentages of H_2.

H_2	**2%**	**6%**	**10%**	**20%**
CH_4 [%]	93.82	90.28	87.00	79.75
O_2 [%]	0.46	0.44	0.43	0.39
N_2 [%]	3.76	3.62	3.48	3.19
H_2 [%]	1.96	5.66	9.09	16.67
LHV [MJ/kg]	46.49	46.84	47.10	46.45

Table 4. Composition of CNG for Different Percentages of H_2.

H_2	**2%**	**6%**	**10%**	**18%**
CH_4 [%]	86.77	83.49	80.45	75.00
C_2H_6 [%]	6.08	5.85	5.64	5.25
C_3H_8 [%]	2.16	2.08	2.00	1.86
C_4H_{10} [%]	0.78	0.75	0.73	0.68
CO_2 [%]	1.76	1.70	1.64	1.53
N_2 [%]	0.49	0.47	0.45	0.42
H_2 [%]	1.96	5.66	9.09	15.26
LHV [MJ/kg]	47.08	47.40	47.71	48.33

2.2 Combustion Model

The calculation of the Mass Fraction Burned (MFB) is essential in the two-zone combustion model. The approach used in this work is the double Wiebe function (equation 1) (Mattos, 2018).

$$\theta_b = p\left(1 - \exp\left[-\frac{\theta - \theta_{b1}}{\Delta\alpha_1}\right]^{\beta_1}\right) + \left(1 - \exp\left[-\frac{\theta - \theta_{b2}}{\Delta\alpha_2}\right]^{\beta_2}\right) \quad (5)$$

The data inserted into the model from Mattos (2018) are derived from experimental simulations of the engine operating with CNG. Subsequently, data from GT-SUITE® are utilized. The data for the double Wiebe function are presented in Table 5, varying the start of combustion (θ_i) and the duration of combustion (θ_b), pressures, and temperatures (intake and exhaust) as a function of each fuel and rotation.

Caption: In this study, p represents the weighting factor applied during two-stage combustion, with a fixed value of 0.5, $\beta_{1,2}$ are shape factors ($m_{1,2}$ +1), $\alpha_{1,2}$ are combustion efficiency coefficients. Index 1 represents complete combustion, and index 2 represents the combustion fraction.

Table 5. Combustion Parameters for Biomethane and CNG.

Fuel	Speed [rpm]	Burn Duration 0-50% (θ_{b1}) [deg]	Burn Duration 50-90% (θ_{b1}) [deg]	Ignition Dealy [deg]
CNG + H_2	2500 3000	31 33	14 14	9.258 10.108
Biomethane + H_2	2500 3000	32 33	14 18	9.258 10.108

2.3 Enter parameters in the phenomenological model

Table 6 shows all the data used in the MATLAB® simulation.

and heavy vehicles. The essential data structure for carrying out exhaust emission calculations is outlined in the flowchart shown in Figure 2.

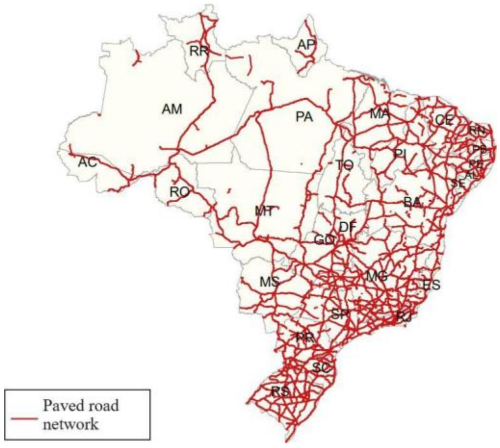

Figure 1. Distribution of the Brazilian road network (IBGE, 2022).

Table 6. Calibration parameters for the MATLAB® code enriched with H_2.

Fuel	Speed [rpm]	Ignition advance [°]	Intake pressure [bar]	Exhaust pressure [bar]	Intake temp.[K]	Exhaust temp. [K]
CNG	2500 3000	-22.00 -20.00	1.60 1.60	1.70 1.80	320.20 319.70	946.00 972.00
Biomethane	2500 3000	-20.00 -17.00	1.60 1.60	1.70 1.80	320.20 319.70	946.00 972.00

2.4 Drawing up the emissions inventory

2.4.1 Characterization of the study area

This study looks at the Brazilian vehicle fleet. Brazil, Latin America's largest country in terms of land area, had a total of 86,692,659 vehicles in 2022, according to data from the National Association of Motor Vehicle Manufacturers (ANFAVEA). These vehicles are divided into four different categories: cars, light commercial vehicles, trucks and buses.-The Brazilian Road network currently covers around 1,720,700 kilometers of roads and highways (Figure 1), and shows a significant concentration in the Center-South areas, notably in the state of São Paulo, which had a fleet of 32,293,191 vehicles in 2022 (MTR, 2022). Table 7 shows the number of light-duty vehicles by fuel type registered in the country in 2022 (ANFAVEA, 2023).

2.4.2. Estimation of exhaust emissions and GHG

The BRAVES model developed by Vasques (2021), offers an approach capable of estimating exhaust emissions for a variety of vehicle categories, covering cars, light commercial vehicles, motorcycles

Table 7. Number of light vehicles registered by type of fuel in Brazil in 2022 (ANFAVEA, 2023).

Fuel	Vehicles [$\times 10^6$]
Diesel	9.15
Gasoline	31.88
Ethanol	5.63
Flex-fuel	39.89

Among the pollutants estimated by BRAVES are methane (CH_4), nitrous oxide (N_2O) and carbon dioxide (CO_2). The magnitude of the emission of these gases is converted into CO_2-eq based on the Global Warming Potential over a 100-year horizon, predicted by the IPCC - Guidelines for National Greenhouse Gas Inventories (IPCC, 2006) and also recommended by the report on vehicle emissions in the state of São Paulo (CETESB, 2022).

3. RESULTS

3.1 Engine performance and emissions

Table 8 shows that, as the percentage of hydrogen in the biomethane mixture increases, both the engine's power and torque decrease, following the same trend as in the work by Kamil and Rahman (2015)

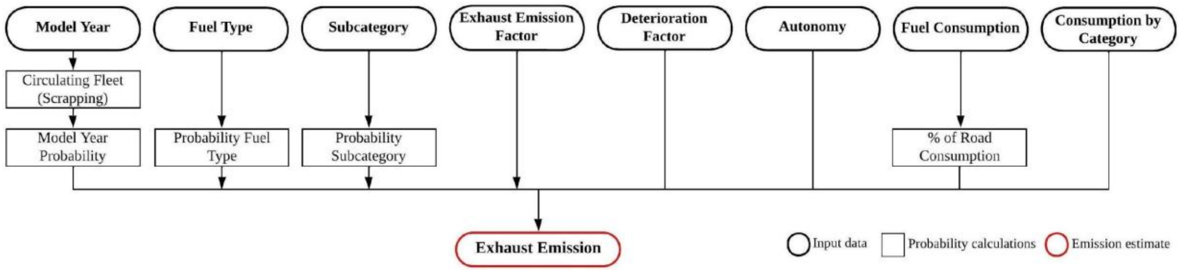

Figure 2. Flowchart of exhaust emission estimates used in BRAVES (Vasques, 2021).

Power varies from 104.84 kW with 2% H_2 to 90.56 kW with 18% H_2, while torque decreases from 400.52 N.m to 345.88 N.m under the same conditions. This trend is consistent with the decrease in energy density when increasing the proportion of hydrogen. The pressure and temperature peaks also decrease as the percentage of hydrogen increases. Suggesting a more efficient and cleaner combustion. Similar observations can be made for performance at 2500 rpm using CNG (Table 9). In this case, power decreases from 95.04 kW to 90.88 kW and torque from 363.04 N.m to 347.16 N.m when increasing the percentage of hydrogen from 2% to 18%.

Caption: *ηt (%)* – Thermal Efficiency, *ηv (%)* – Volumetric Efficiency, and *ISFC (g/kW·h)* – Indicated Specific Fuel Consumption.

Table 8. Engine performance data with different Biomethane and H_2 mixtures at 2500 rpm.

Speed 2500 rpm	2% H_2	6% H_2	10% H_2	18% H_2
η_t (%)	40.04	39.92	39.85	39.83
η_v (%)	130.74	130.98	131.35	131.78
Power (kW)	104.84	98.36	94.48	90.56
Torque (N.m)	400.52	375.68	360.92	345.88
Peak pressure (p) (bar)	123.90	116.30	113.10	109.80
Peak burned temperature (Tb) (K)	2746.00	2592.00	2524.00	2452.00
ISFC (g/kW.h)	194.43	193.55	192.86	191.48

Table 10 shows that, at 3000 rpm, the engine's power when using biomethane varies from 128.52 kW with 2% H_2 to 109.28 kW with 18% H_2.

The torque decreases from 409.04 N.m to 345.28 N.m when increasing the proportion of hydrogen. Again, the pressure and temperature peaks follow a downward trend. Table 11 shows similar results for CNG blends at 3000 rpm, where power varies from 108.56 kW to 102.80 kW and torque from 345.48 N.m to 327.28 N.m when increasing the proportion of hydrogen.

Increasing the concentration of H_2 in blends with biomethane and CNG progressively reduces the peak pressure (Peak p) in the cylinders, as can be seen in the tables. In the case of biomethane at 2500 rpm, the peak pressure drops from 123.9 bar with 2% H_2 to 109.8 bar with 18% H_2, accompanied by a drop in combustion temperature (Peak Tb) and power (from 104.84 kW to 90.56 kW). A similar trend can be seen with CNG at 2500 rpm, where the peak pressure drops from 122.1 bar to 105.3 bar. The reduction in peak pressure is due to the decrease in energy content per unit volume of the fuel with the addition of hydrogen (Ji and Wang (2010).

Table 9. Engine performance data with different CNG and H_2 mixtures.

Speed 2500 rpm	2% H_2	6% H_2	10% H_2	18% H_2
η_t (%)	40.53	40.52	40.45	39.96
η_v (%)	135.34	135.20	131.96	131.16
Power (kW)	95.04	94.60	92.20	90.88
Torque (N.m)	363.04	361.36	352.20	347.16
Peak p (bar)	122.10	111.10	107.30	105.30
Peak Tb (K)	2343.00	2230.00	2179.00	2164.00
ISFC (g/kW.h)	188.67	186.26	184.21	182.16

Table 10. Engine performance data with different Biomethane and H_2 mixtures at 3000 rpm.

Speed 3000 rpm	2% H_2	6% H_2	10% H_2	18% H_2
η_t (%)	39.61	39.46	39.43	39.41
η_v (%)	134.03	134.83	135.29	135.88
Power (kW)	128.52	117.84	113.28	109.28
Torque (N.m)	409.04	375.08	360.52	345.28
Peak p (bar)	113.00	106.30	103.50	100.50
Peak Tb (K)	2500.00	2349.00	2283.00	2213.00
ISFC (g/kW.h)	196.51	194.71	193.71	191.53

At 3000 rpm, for both biomethane and CNG, the addition of H_2 continues to reduce the peak pressure. This reduction results in lower torque and power, but also improves specific fuel consumption (ISFC).

Thus, reducing peak pressure smooths combustion and can reduce the risk of detonation, but the drop in engine performance is evident.

Table 11. Engine performance data with different CNG and H_2 mixtures at 3000 rpm.

Speed 3000 rpm	2% H_2	6% H_2	10% H_2	18% H_2
η_t (%)	40.14	39.81	39.52	39.45
η_v (%)	132.80	132.70	132.64	102.80
Power (kW)	108.56	107.24	106.40	102.80
Torque (N.m)	345.48	341.40	338.64	327.28
Peak p (bar)	107.80	98.31	97.51	92.04
Peak Tb (K)	2452.00	2327.00	2234.00	2130.00
ISFC (g/kW.h)	190.48	189.60	188.52	127.69

With regard to CO emissions, it was observed that, for CNG at 2500 rpm, blends with 2% hydrogen had the highest emissions, followed by blends with 6%, 10% and 18% hydrogen, respectively. This trend indicates that adding higher proportions of hydrogen to CNG can reduce CO emissions. Similarly, a similar trend was seen for biomethane at 3000 rpm, where CO emissions decreased as the percentage of hydrogen in the blend increased. These observations can be seen in Figures 3 and 4, which show the inverse relationship between the proportion of hydrogen in the fuel mixtures and CO emissions. The same trend occurs in the work by (Park *et al.* (2011)) and (Pandey *et al.* (2023).

The reduction in CO emissions with an increase in the proportion of hydrogen is due to its high flame speed and wide flammability range. Hydrogen improves combustion efficiency by increasing the availability of oxygen and reducing the formation of CO, which results from incomplete combustion. Thus, the higher the proportion of hydrogen, the lower the CO emissions (Li *et al.* (2024)). In Figures 5 and 6, it can be observed that NOx values follow the same trend across all tested engine speeds.

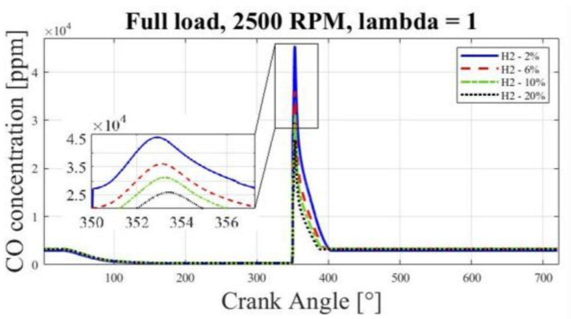

Figure 3. CO emissions for CNG at 2500 rpm

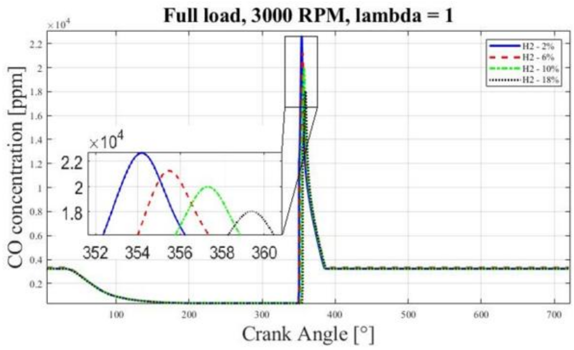

Figure 4. CO emissions for Biomethane at 3000 rpm.

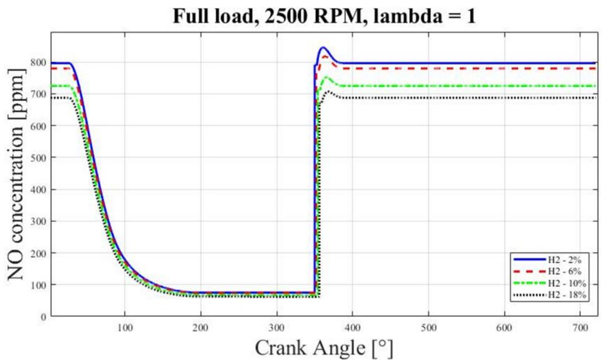

Figure 5. NO_x emissions for CNG at 2500 rpm.

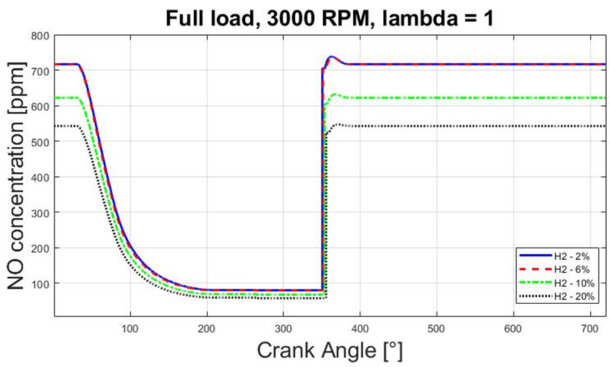

Figure 6. NO_x emissions for Biomethane at 3000 rpm.

3.2 Emissions inventory

Vehicular emissions estimated by BRAVES for the operation of the F1-C engine in Brazil are presented in Figure 7. The study results indicate that the combination of CNG with 18% H_2 can reduce emissions by up to 4.67%, while biomethane with 20% H_2 shows a decrease of 5.54%. In the case of CNG, the addition of hydrogen in different proportions (2%, 6%, 10% and 18%) generates reductions in CO_{2-eq} emissions of 0.53%, 1.57%, 2.59% and 4.67%, respectively. For biomethane, the equivalent reductions are 0.59%, 1.78%, 2.55% and 5.54%, with the addition of 2%, 6%, 10% and 20%

H_2, respectively. When comparing the two fuels, the use of biomethane (with 20% H_2) reduces CO_{2-eq} emissions by up to 4.94% compared to CNG (with 18% H_2). In addition, for hydrogen compositions of 2%, 6% and 10% in biomethane, CO_{2-eq} emission reductions of 4.19%, 4.34% and 4.05%, respectively, were observed. These results indicate that the incorporation of hydrogen into biomethane can significantly contribute to the reduction of GHG emissions compared to CNG.

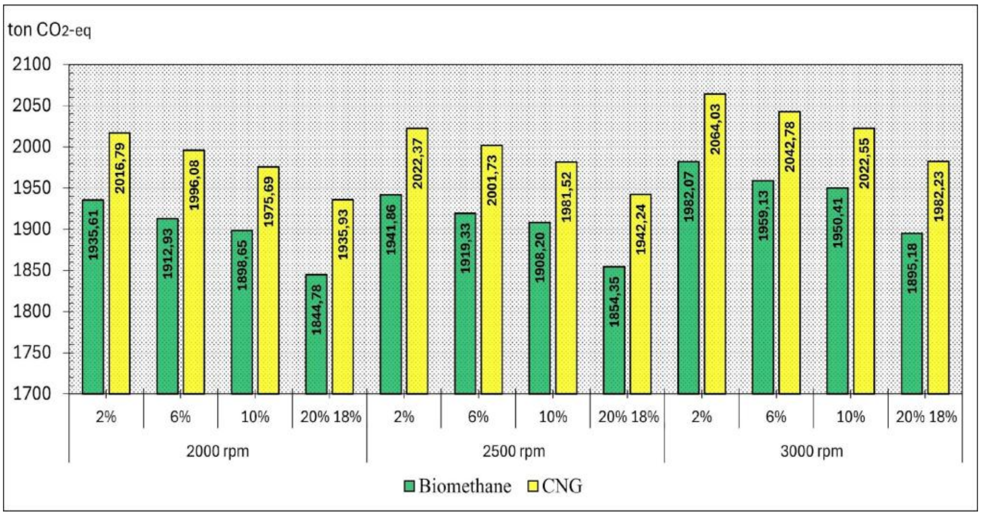

Figure 7. Estimation of total vehicle emissions of CO_{2-eq} for CNG and Biomethane fuels with different additions of H_2.

4. CONCLUSION

- Increasing the percentage of hydrogen in biomethane and CNG blends results in a consistent decrease in engine torque. The same occurs with engine power, which decreases significantly as the proportion of hydrogen in biomethane and CNG blends increases, demonstrating a direct relationship between the greater presence of hydrogen and the reduction in power generated.

- Reduction in CO emissions: Increasing the proportion of hydrogen in the fuel mixtures resulted in lower carbon monoxide (CO) emissions, indicating more complete combustion. Hydrogen improves combustion efficiency by reducing CO formation. Increase in NO_x Emissions: For both CNG at 3000 rpm and biomethane at 2500 rpm, NO_x emissions were higher with the addition of 2% hydrogen, gradually decreasing with higher hydrogen concentrations. CNG had almost double the NO_x emissions compared to biomethane, reflecting a significant difference between the two fuels.

- Reduction in CO_{2-eq} emissions: Incorporating hydrogen into biomethane fuel can reduce CO_{2-eq} emissions by up to 5.5%, offering a promising path to substantially reduce GHG emissions compared to CNG.

- Difference Between Fuels: CNG showed a more pronounced impact on NO_x emissions compared to biomethane, due to the higher concentration of nitrogen and oxygen in CNG that contributes to the formation of NO_x during combustion.

5. ACKNOWLEDGEMENTS

The authors would like to acknowledge the aid and financial support provided by Fundação de Desenvolvimento da Pesquisa – Fundep Rota 2030/Linha V (Proc. No 27192*62).

6. REFERENCES

ANFAVEA, 2023. “Anuário da indústria automobilística brasileira”. *Associação Nacional dos Fabricantes de Veículos Automotores*.

Barin, I. and Platzki, G., 1989. *Thermochemical Data of Pure Substances*, Vol. 304. Wiley Online Library.

CETESB, 2022. “Emissões veiculares no estado de São Paulo 2020”. *CETESB - Companhia Ambiental do Estado de São Paulo*.

Empresa de Pesquisa Energética, 2024. “Balanço Energético Nacional”.

IBGE, 2022. “Cidades e estados”. *Instituto Brasileiro de Geografia e Estatística*.

IPCC, 2006. “Ipcc guideline for national greenhouse gas inventories. chapter 3: Mobile combustion”. *Intergovernmental Panel on Climate Change*.

Ji, C. and Wang, S., 2010. “Experimental study on combustion and emissions performance of a hybrid hydrogen–gasoline engine at lean burn limits”. *International Journal of Hydrogen Energy*, Vol. 35, No. 3, pp. 1453–1462. ISSN 0360-3199. doi:https://doi.org/10.1016/j.ijhydene.2009.11.051. URL https://www.sciencedirect.com/science/article/pii/S0360319909018205.

Kamil, M. and Rahman, M., 2015. “Performance prediction of spark-ignition engine running on gasoline-hydrogen and methane-hydrogen blends”. *Applied Energy*, Vol. 158, pp. 556–567. ISSN 0306-2619.

Li, B., Zhong, F., Wang, R., Jiang, Y. and Chen, Y., 2024. “Experimental and numerical study on a si engine fueled with gasohol and dissociated methanol gas blends at lean conditions”. *Energy*, Vol. 292, p. 130540.

Mattos, A.P., 2018. *Estudo do desempenho de um motor turbo alimentado a etanol empregando EGR para redução de emissões de NOx e controle de detonação*. Ph.D. thesis, Universidade Estadual de Campinas, Faculdade de Engenharia Mecânica.

MTR, 2022. “Frota de veículos - 2022”. *Ministério dos Transportes*.

Pandey, V., Shahapurkar, K.H., Guluwadi, S., Mengesha, G.A., Gadissa, B., Banapurmath, N.R., Vadlamudi, C., Krish- nappa, S. and Khan, T.M.Y., 2023. “Studies on the performance of engines powered with hydrogen-enriched biogas”. *Energies*, Vol. 16, No. 11. ISSN 1996-1073. URL https://www.mdpi.com/1996-1073/16/11/4349.

Park, C., Kim, C., Choi, Y., Won, S. and Moriyoshi, Y., 2011. “The influences of hydrogen on the performance and emission characteristics of a heavy duty natural gas engine”. *International Journal of Hydrogen Energy*, Vol. 36, No. 5, pp. 3739–3745.

Urroz, J.C., Diéguez, P.M., Arzamendi, G., Arana, M. and Gandía, L.M., 2023. “Gaseous fueling of an adapted com- mercial automotive spark-ignition engine: Simplified thermodynamic modeling and experimental study running on hydrogen, methane, carbon monoxide and their mixtures”. *Fuel*, Vol. 337, p. 127178.

Vasques, T.V., 2021. “Inventário de emissões veiculares no brasil: Brazilian vehicular emission inventory software - braves”. *UFSC*.

Yıldız, M. and Albayrak Çeper, B., 2017. “Zero-dimensional single zone engine modeling of an si engine fuelled with methane and methane-hydrogen blend using single and double wiebe function: A comparative study”. *International Journal of Hydrogen Energy*, Vol. 42, No. 40, pp. 25756–25765.

7. RESPONSIBILITY NOTICE

The authors are solely responsible for the printed material included in this paper.